Improved Space Object Observation Techniques using CMOS Detectors

T. Schildknecht[(1)], A. Hinze[(1)], P. Schlatter[(1)], J. Silha[(1)], J. Peltonen[(2)], T. Säntti[(2)], T. Flohrer[(3)]

[(1)] Astronomical Institute, University of Bern, Sidlerstrasse 5, CH-3012 Bern, Switzerland,
Email: thomas.schildknecht@aiub.unibe.ch, andreas.hinze@aiub.unibe.ch
[(2)] Aboa Space Research Oy (ASRO), Turku, Finland, Email: juhpe@asro-space.com, teansa@asro-space.com
[(3)] Space Debris Office, ESA/ESOC, Germany, Email: tim.flohrer@esa.int

ABSTRACT

CMOS-sensors, or in general Active Pixel Sensors (APS), are rapidly replacing CCDs in the consumer camera market. Due to significant technological advances during the past years these devices start to compete with CCDs also for demanding scientific imaging applications, in particular in the astronomy community. CMOS detectors offer a series of inherent advantages compared to CCDs, due to the structure of their basic pixel cells, which each contain their own amplifier and readout electronics. The most prominent advantages for space object observations are the extremely fast and flexible readout capabilities, feasibility for electronic shuttering and precise epoch registration, and the potential to perform image processing operations on-chip and in real-time.

Presently applied and proposed optical observation strategies for space debris surveys and space surveillance applications had to be analyzed. The major design drivers were identified and potential benefits from using available and future CMOS sensors were assessed.

The major challenges and design drivers for ground-based and space-based optical observation strategies have been analyzed. CMOS detector characteristics were critically evaluated and compared with the established CCD technology, especially with respect to the above mentioned observations. Similarly, the desirable on-chip processing functionalities which would further enhance the object detection and image segmentation were identified.

Finally, the characteristics of a particular CMOS sensor available at the Zimmerwald observatory were analyzed by performing laboratory test measurements.

1 OPTICAL SPACE OBJECT OBSERVATION STRATEGIES

In order to assess the potential benefits of current and future CMOS detectors for space observations, the presently applied and proposed optical observation strategies for space debris surveys and space surveillance applications had to be analyzed. Optical space objects observation techniques may be arranged in two classes, the techniques which are used to search for unknown objects by performing so-called surveys and the so-called tasked observation where known objects are followed up to refine or maintain their orbits or to further characterize them. While tasked observations use rather similar observation scenarios for all different orbit regimes, usually the objects are simply tracked by using an ephemeris computed from an orbit of the known object, survey scenarios my vary considerably depending on the orbit region to be surveyed. Observation scenarios for ground-based optical surveys of the geostationary orbit (GEO) region have been presented in, e.g., [1], [3], and [4], survey techniques for the Geostationary Transfer Orbit (GTO) region were addressed in [2], and for the region of the global navigation satellite systems (Medium Earth Orbits, MEO) in [4]. There is very limited literature discussing ground-based optical survey techniques for objects in Low Earth Orbits (LEO) (see e.g. [5]).

Space-based observations of objects have been proposed for two different applications, the surveillance of high-altitude objects from a platform in a LEO orbit with the aim to support orbit catalogues ([6]), and the short range observations of small-size debris in different orbital regimes in support improving and validating of statistical debris models ([7]).

During optical surveys in any kind of orbital region a series of consecutive frames is acquired while an object is crossing the field of view (FoV) of the telescope. Observations of one and the same object on such a series of frames form a short arc and are associated to a so-called tracklet. In order to reduce the false association rate within a tracklet, a minimum of three consecutive observations during a single FoV-crossing is required. Tracklets spanning a long time interval are preferred for the orbit determination and for the "tracklet-to-tracklet" association task. Consequently the FoV-diameter should be "as wide as possible". Wide fields are also of interest to maximize the sky area covered per time interval by a single telescope.

Many survey scenarios are based on so-called scanning fences were the telescope is moved in between series of exposures in order to form a fence with a width of one FoV and a certain length. If the fence should be "leak-

proof" the scenario has to guarantee that each field of the fence is re-observed at least once per typical FoV dwell time of the objects of interest.

The optimum exposure time for such observations is of the order of a few times the time interval it takes for an object to cross a single pixel of the sensor (pixel dwell time). Depending on the angular velocity of the objects exposure times may range from a few milliseconds to a few seconds.

One important issue to consider, is the fact that the actual epochs of the exposures must be determined with an accuracy corresponding to the required astrometric accuracy. This requires an accurate registration of these epochs, which in turn includes the entire chain from the shuttering (electronic or mechanical), to the clock used.

1.1 Requirements for imaging sensor

In order to minimize the sensor dead-time the detector readout rate should be as high as possible. Ideally the time required to readout the sensor should be negligible when compared with the integration time. Ground-based observations of objects in LEO and short range space-based observations face short FoV dwell times due to the high angular velocities of the objects. In these cases short readout times are absolutely mandatory.

Table 1 summarizes the main characteristics of ground-based space object observations assuming a telescope FoV of 3° and the corresponding detector requirements. The red shaded cells indicate requirements which are difficult to be fulfilled by classical CCD detectors. In particular the very demanding epoch accuracy of less than a millisecond in case of LEO observations can only be obtained with electronic shutters. LEO observation scenarios also require extremely short readout times and would perhaps benefit from non-destructive readout capabilities.

Space-based observations using a sensor in LEO to observe objects in GEO or MEO have similar characteristics as the corresponding ground-based observations and thus the same detector requirements. Short-range observations (e.g. to search for small space debris) using a space-based sensor are in terms of detector requirements comparable to the ground-based LEO case. A mechanical shutter is not advisable for any sensor in space. All space sensors would benefit from on-board or even on-chip (i.e. on detector) processing to reduce downlink bandwidth requirements.

Table 1. Main characteristics of ground-based space object observations and the corresponding detector requirements (epoch accuracy set not to compromise expected astrometric accuracy). Red shaded cells indicate requirements which are difficult to be fulfilled by classical CCD detectors.

	Ground-based GEO	Ground-based MEO/GTO	Ground-based LEO
Angular velocity of objects	< 20"/s	<100"/s	200"/s – 1800"/s
FoV dwell time (3° FoV)	540s @20"/s	108s @100"/s	~ 6s @1800"/s
Epoch accuracy (0.5")	25ms	5 ms	0.28ms
Exposure time	10 s ≥ 1s	10 s ≥ 1s	<<1s
Detector readout	few sec	few sec	<<1s; (non-destructive)
Processing			streak det.
Electronic shutter	desired	desired	required

In addition to these specific requirements the following generic detector requirements hold for all space object observations:

- high quantum efficiency
- low read-out noise
- low dark current
- stable flat field (i.e. stable gain for each pixel)
- stable bias or on-chip bias reduction
- limited number of dark/hot pixels ("cosmetics")
- no charge leakage from pixel to pixel
- limited enlargement of point-spread-function
- high full-well capacity

A list of specific requirements for a future imaging sensor which is optimized for space object observations is given in Table 2.

Table 2. Requirements for an imaging sensor optimized for space object observations.

Electronic shutter - required for space-based sensor - required for precise epoch registration (surveys LEO) - increased reliability for ground-based sensors
Faster read-out (large sensors!) - improved duty cycle ▪ larger survey area are per time - more observations per tracklet (FoV crossing) ▪ improved orbit accuracy ▪ improved tracklet correlation
Extremely short exposures <<1s - required for ground-based LEO and space-based short range observations - non-destructive readout to "subdivide" streaks
On-chip parallel processing - potential applications ▪ spatial filtering ▪ image segmentation

2 CMOS IMAGING SENSORS

CMOS-sensors or Active Pixel Sensors (APS) are rapidly replacing CCDs in the consumer camera markets. The main difference between CMOS-imager and CCD detector lies in the structure of their basic pixel cells and in the manufacturing process. The CCD pixel consists of relatively simple, transparent patterns manufactured on the surface of a silicon wafer. The transfer of charges to the output amplifiers of the chip is done in CCD by the help of external electronics, while the internal structure of the CCD cells is kept simple. In comparison the cells of CMOS-imagers include much more structures: elemental signal amplification and circuits for charge transfer (multiplexing) are integrated on the surface of the pixel.

In CMOS every pixel has its own amplifier with manufacturing variations, radiation and temperature drifts. The Pixel Response Non-Uniformity (PRNU) of CMOS detectors can therefore be a serious issue for astrometric and photoemtric measurements. Other problems of CMOS include low field strengths, pixel to pixel leakage and typically slightly lower QE than for CCDs. On the positive side, the power consumption of CMOS is negligible when compared with the CCDs, and complex electronics can be included on the same wafer with the sensor elements.

As with the CCDs, there are many variations of the basic CMOS concept. The variations include the pixels themselves, amplifiers, the row/column read-out, and supporting electronics. CMOS-sensors also come as front- and back- illuminated. The basic principle of the front illuminated CMOS sensor is the same as with CCDs with the exception that the area of the pixels is filled also with transistors and conductors resulting in a small fill factor and thus lower quantum efficiency than for front illuminated CCDs. Consequently microlenses are often used for performance improvements. Microlenses may, however, result in optical crosstalk if the numerical aperture (NA) of the optical system is not matching the numerical aperture of the microlenses as shown in Figure 1 (right).

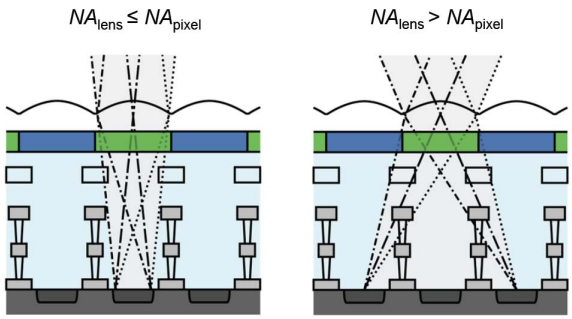

Figure 1. Optical crosstalk produced by microlenses (from [9]).

Hybrid detectors combine a matrix of photodiodes with a matrix of CMOS multiplexers/amplifiers. Both are processed separately. The contact between the pixels and CMOS readout (ROIC) is done by bump bonding (pixel to pixel). There are thus millions of tiny connections between the two matrixes.

The photodiode can be optimised for the wanted light frequency and manufactured with a fill factor of ~100%. Special coatings can be used for reduced light scattering. Each of the pixel amplifiers can be optimised more freely than in the case of CMOS imagers, because obscuring the path of light to the sensitive volume of the silicon is not an issue. These hybrid detectors can in principle have the best of both: the sensitivity of the CCDs and the ease of use of the CMOS detectors. However, there are some technical issues like the increased capacitance and cross talk at the pixel readout node, the complexity of manufacturing and then, the price: The manufacturing of devices with millions of connections is still difficult and very expensive.

2.1 Electronic shutter

CMOS imagers have electronic shutters by definition and can be read out in either rolling shutter or global shutter mode. In the rolling shutter mode the readout "rolls" line by line across the active area resulting in a different exposure epoch for each row. For space object observations a global shutter is thus mandatory. The disadvantages of global shutters are that they require an intermediate storage at pixel level, have a higher readout noise, and a limited extinction ratio of 1-0.1%. The electronic shuttering and readout circuits allow almost arbitrary short exposure times, duty cycles of 100% (i.e. integration during readout), non-destructive readout of accumulated charge, and registration of effective exposure epochs with a precision of far less than one millisecond.

2.2 On-chip processing

CMOS imagers allow monolithic integration of readout and signal processing on the same chip. A sensor can integrate various signal and image processing blocks such as amplifiers, ADCs, circuits for image processing and data compression. In particular algorithms which require massive pixel parallel processing may benefit from on-chip processing hardware.

Classical examples would be spatial filters which assign new values for each pixel taking into account the actual value of the pixel and the values of adjacent pixels. The commercial sCMOS device discussed in Section 3 uses this technique to assign interpolated values to identified "bad" pixels (see Section 3.3). Algorithms used to find faint space objects on digital frames often convolve the image with the point-spread-function of the sensor in order to maximize the signal-to-noise ratio, another ex-

ample for a processing step which would benefit from parallel processing.

If local pixel storage for reference values can be established, background subtraction and simple image segmentation processes are additional candidates to be implemented in CMOS detectors. Furthermore paralleled, application specific image processing pipelines could be integrated on the same chip outside the active area.

CMOS devices allow complex random access and windowing of image data including continuous and non-destructive readout. These features would, e.g., allow subdividing trails from moving objects during the exposure and active tracking of regions of interest (moving objects, reference stars, etc.).

2.3 Comparison of silicon-based imaging sensors

A summary of the main advantages and disadvantages of different silicon-based imaging sensors to be used for the optical observations of space objects is given in Table 3.

Table 3. Main advantages (green) and disadvantages (red) of different silicon-based imaging sensors.

	CCD	sCMOS	Hybrid CMOS
Quantum eff. (@500nm)	>90% (thinned)	60% with microlenses	>90%
Read noise	6-10e$^-$ @1MHz	<2e$^-$ @560MHz	7-10e$^-$ @1MHz
Dynamic range	1:10-20 000	1:16 000	~1: 5 000
Uniformity	good	fair	fair
p2p cross-talk	some	some?	some extra
Fast readout	<1fps	30-60 fps	30-60 fps
Electronic shutter	(yes)	rolling/global	rolling
Radiation tolerance.	fair/good	?	good
Complex readout	no	random access; non.-destructive	random access; non.-destructive
Processing	no	limited on-chip	side-car

3 CHARACTERIZATION OF AN SCMOS CAMERA

Currently there are only very few scientific CMOS cameras commercially available. In order to characterize one of the commercially available CMOS sensors, laboratory tests with an Andor Neo camera were performed at the Zimmerwald observatory. This camera is built around the CMOS sensor CIS2051 developed by the companies Andor Technology (Northern Ireland), Fairchild Imaging (USA, now a division of BAE Systems), and PCO AG (Germany) [1]. The sensor is aimed at scientific applications, hence the designation sCMOS (scientific CMOS). Two particular features are the high frame rate combined with a low read noise and the choice of rolling or global shutter operation. Depending on the operating mode, burst frame rates range from 100 fps for a 5.5 Mpixel image to 1760 fps for a sub-frame of 128x128 pixels. The main characteristics of the sensor are summarized in Table 4.

Table 4. Main characteristics of Andor Neo camara.

Sensor format	2560 (h) x 2160 (v) pixels
Pixel size	6.5 µm x 6.5 µm
Pixel readout rate (MHz)	560, 200
Read noise	<2 e$^-$ to <15 e$^-$ (depending on operating mode)
Full-well capacity	30'000 e$^-$
Dynamic range	600 to 16'000 (depending on operating mode)
Quantum efficiency	<60% at 550 nm

A schematic view of the sensor is given in Figure 2. The sensor is split into an upper and a lower half, and every half has its own readout circuits. The charge collected by every pixel is converted into a voltage by a 5-transistor design. The voltages are amplified and converted by column level amplifiers and ADCs which are shown in an expanded view in Figure 3.

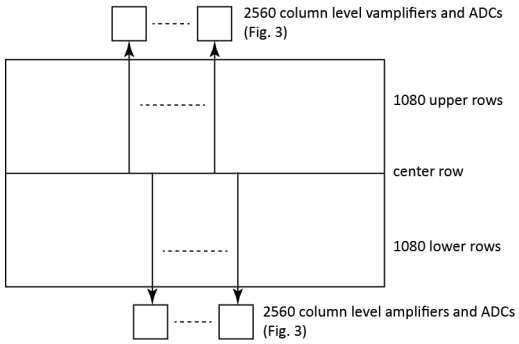

Figure 2. Schematic view of the sensor. The pixels are read out starting from the centre row towards the top and bottom edge of the sensor, as indicated by the arrows.

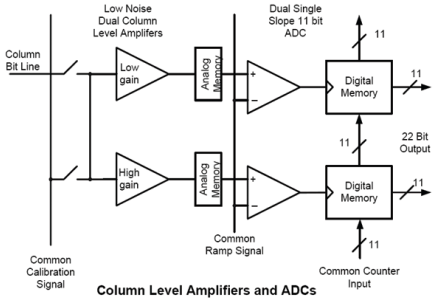

Figure 3. Column level amplifiers and ADCs (from [10]).

The choice of high- or low-gain amplifier is up to the user. In the low-gain mode, the full-well capacity of the pixels may be fully exploited with the drawback of higher read noise, whereas in the high-gain mode the read noise is low but the dynamic range is limited by the ADC. The sensor offers a dual-gain mode where the signal passes through one of the amplifiers depending on the signal level. Low noise and high dynamic range are available at the same time.

3.1 Read Noise

For a CMOS sensor, the read noise is not a global property like for CCDs. It must be measured for every individual pixel by taking a large number of bias frames. As a consequence a CMOS sensor is not characterized by a single global read noise value but by a read noise distribution. The read noise has been determined by taking 1000 bias frames of 512x512 pixels. Figure 4 shows the signal level distribution of two individual pixels.

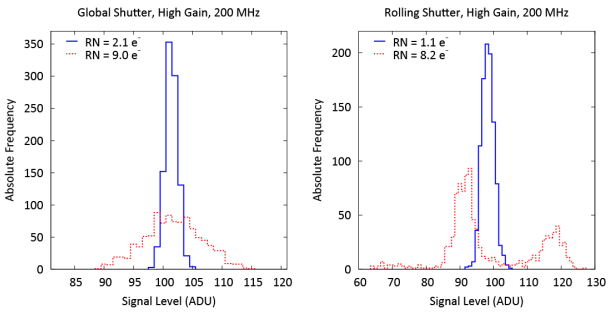

Figure 4. Distribution of the signal levels of two individual pixels based on 1000 bias images.

The read noise, i.e. the standard deviation of the signal level distribution, varies considerably from pixel to pixel. For global shutter mode, the bias signals of low and high noise pixels are normally distributed (left part of Figure 4 whereas in rolling shutter mode the high noise pixels often exhibit a double peaked distribution (right part of Figure 4). So far, there is no explanation for this behavior.

The distribution of the read noise of all 512x512 pixels is shown in Figure 5. The read noise is distributed over a wide range in contrast to the very narrow, Gaussian read noise distribution of a CCD. The red curve represents the noise values of a hypothetical, CCD-like sensor with identical pixels and a read noise of 1.8 e^- and a standard deviation of $1.8/(2(m\text{-}1))^{1/2}$, where m=1000 is the number of bias images.

Due to the extended tail towards high noise values a bias frame is interspersed with bright pixels. For certain applications, e.g. the photometry of weak point-like sources, it is important to pay attention to the high-noise pixels. In the example considered here, one pixel in a sub-array of only 10x10 pixels will, on average, exhibit a read noise that is 5 times higher than the median value.

3.2 Non-Linearity

The non-linearity and the transfer curves were determined with a flat-field screen illuminated by a LED array driven with a constant current source. The measurement equipment was placed in a room held at constant temperature in order to avoid temperature drifts of the light output. During a measurement cycle, the light output of the LEDs changed by less than 0.5%. The signal level was varied by adjusting the exposure time of the camera. Due to the nature of the electronic shutter exposure times are expected to be very precise. Short image sequences with a constant exposure time didn't reveal any sign of signal variation beyond the expected stochastic variation. The signal variance in the transfer curves was determined by taking the difference between two flat-field frames.

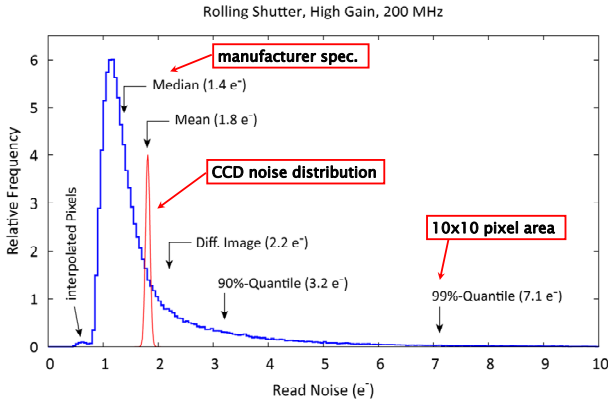

Figure 5. Distribution of the read noise over 512x512 pixels (high gain mode; for the red curve see text).

The non-linearity and transfer curves of the high and the low gain modes are shown in Figure 6 and Figure 7.

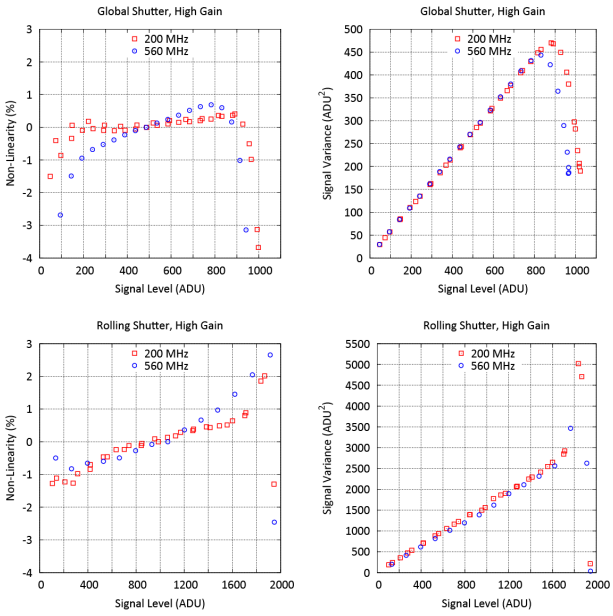

Figure 6. High gain modes. Left: non-linearity, right: transfer curves, top: global shutter, bottom: rolling shutter.

The transfer curves are linear to the point of saturation and the non-linearity is more or less within the advertised range of ±1%. But there is one important exception for the high gain modes, where only one of the two 11-bit ADCs is active. With an average bias value of ~100 ADU the unbiased signal should run into AD-saturation at about 2^{11}-100 = 1900 ADU (the full-well capacity is never reached in high gain modes). This is true for the rolling shutter mode, but the global shutter breaks down at 900 ADU. A factor of two in dynamic range is wasted. Andor recognizes that this is a deficiency of the sensor.

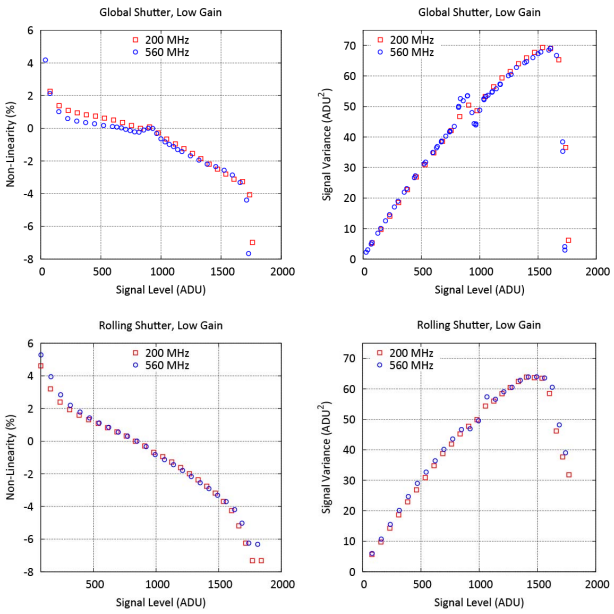

Figure 7. Low gain modes. Left: non-linearity, right: transfer curves, top: global shutter, bottom: rolling shutter.

The low gain modes are designed such that the pixels reach full-well capacity somewhat below the 11-bit ADC saturation level. The non-linearity is distinctly larger than with high gain modes. This is not surprising since the exposure times are longer and the pixels are charged with more electrons. But the sensor clearly misses the advertised non-linearity of ±1%.

The transfer curves show two peculiarities. Even at low signal levels the curves bend and at about half-saturation the variance behaves very strangely. The bending of the curves may be caused by the non-linearity of an amplifier stage. But for the bumpy structure at half-saturation there is currently no explanation.

The dual gain modes employ a very demanding technique. Depending on the signal level, for every half-column either the high gain or low gain path is chosen. The digital high gain (low intensity) signal remains unaffected while the low gain (high intensity) signal is digitally multiplied by a factor that equals the ratio of the analog high gain to low gain amplification. Andor state in their latest brochure [11]:

"Due to the splicing together of the low and high gains, the transition region between them is not seamless but has been optimized as far as possible."

The problems become obvious when looking at Figure 8. The transfer curve shows the same bumpy structure at half-saturation as with the low gain modes. In addition, the transition region between the low and high gain path is clearly visible at 1000 ADU for the global shutter mode and at 2000 ADU for the rolling shutter mode. One of the operating modes (global shutter, dual gain, 560 MHz) is completely out of tolerance.

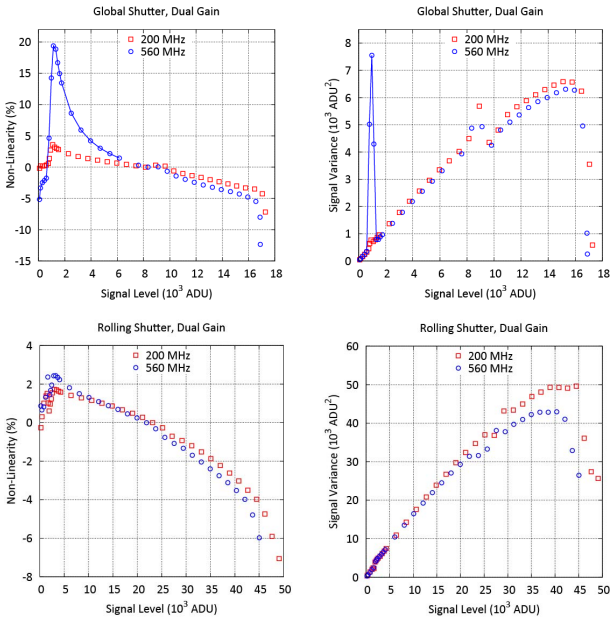

Figure 8. Dual gain modes. Left: non-linearity, right: transfer curves, top: global shutter, bottom: rolling shutter.

If the difference between two flat-field frames is taken and only the pixels that passed the low-gain channel are selected it can be demonstrated that the signal levels have been digitally multiplied by a factor of about 10, see Figure 9. This factor is (or should be) equal to the ratio of the high- to low-gain analog amplification. The comb structure becomes apparent in all dual gain modes when the difference of two flat-field frames is taken. In principle, the comb structure should already be visible in a single flat-frame but it is hidden behind fixed-pattern noise. The combined 16-bit signal of a dual-mode image carries less information than a signal produced by a single 16-bit ADC.

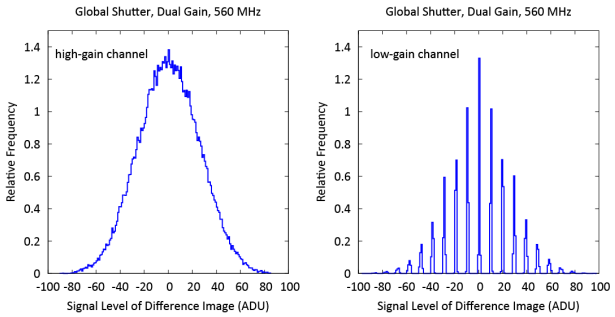

Figure 9. Distribution of the signal levels in the difference frame of two flat-fields. Left: Signals that passed the high-gain channel. Right: Signals that passed the low-gain channel and that were digitally multiplied by 10.

3.3 Interpolated pixels

Another peculiarity of the camera is revealed by the distribution of the individual pixel variances estimated from 1000 flat-field frames (Figure 10). There is a well separated population of pixels with a variance that is exactly 8 times less than the average of the main population. The reason is that about 0.9% of the pixels are interpolated from the 8 neighbors. Presumably, these pixels are either dead or very hot. Both rolling and global shutter modes have about the same amount of interpolated pixels. The sets are not identical but there is some overlap. It is important to note that on average there is one such interpolated pixel in a 10x10 pixel array.

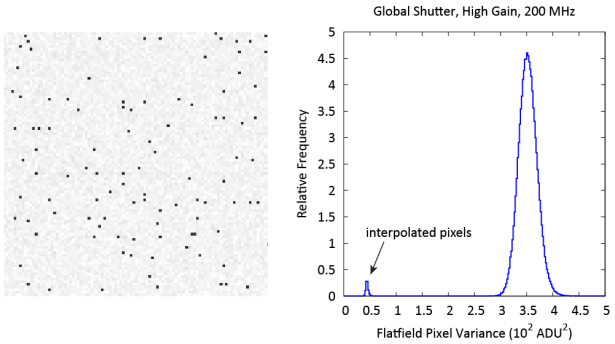

Figure 10. Distribution of the flat-field variance over 512x512 pixels. The individual pixel variances were determined from a series of 1000 flat-field frames. Left: 2D-image of variances, small variances are rendered dark. Right: Distribution of variances.

3.4 Pixel to pixel cross-talk

Autocorrelation analysis is a tool for revealing crosstalk between pixels [12]. Causes for crosstalk are capacitive coupling between pixels and the spreading of charge over neighboring pixels, e.g. when a photon hits the sensor at a shallow angle (see Figure 1). Pixel crosstalk acts as a low-pass filter and reduces the resolution of a sensor. It also affects the transfer function and hence the determination of the conversion factor [13].

Figure 11 shows horizontal and vertical traces of the 2D autocorrelation of flat-field difference images. The Neo sensor is compared to a CMOS sensor of a commercial digital camera where the raw pixel data of the green channel have been read out. The pixels of the consumer camera are uncorrelated, whereas the neo sensor exhibits some weak correlation. The vertical trace reveals a minor low-pass characteristic, corresponding to a cross-talk between neighboring pixels of ~0.5%. In the horizontal direction, the correlation attains a constant value of about 1% over the full width of the sensor. There is so far no explanation for this behavior.

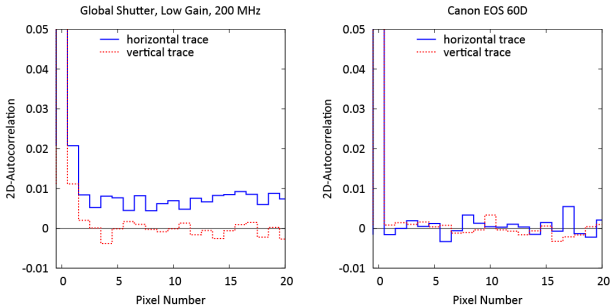

Figure 11. Horizontal and vertical traces of a 2D flat-field autocorrelation. The autocorrelation is normalized to 1 at pixel number 0. Left: Andor Neo camera. Right: Canon EOS 60D camera, raw data of green channel.

4 CONCLUSIONS

The major challenges and design drivers for ground-based and space-based optical observation strategies have been analyzed. We mapped needs from currently applied and discussed observation strategies to detector requirements. The most prominent challenge is the ability to detect fast moving, faint objects in front of the stellar background on images taken by wide-field sensors. Optical observations of space objects require an imaging sensor with fast readout, the possibility to perform short exposures and to precisely register the epochs of the exposures. Ground-based observations of objects in the LEO region and space-based short range observations are particularly demanding. For these applications sensors with electronic shutters and extremely high readout rates are mandatory, and some on-chip processing capabilities would be highly beneficial.

CMOS detectors offer a series of inherent advantages compared to CCDs, due to the structure of their basic pixel cells, which each contain their own amplifier and readout electronics. The most prominent advantages for space object observations are the extremely fast and flexible readout capabilities, feasibility for electronic shuttering and precise epoch registration, and the potential to perform image processing operations on-chip and in real-time.

CMOS sensors have still some inherent disadvantages compared to classical CCD detectors. They suffer from different noise sources which set the fundamental limits of their performance, their pixel to pixel sensitivity variation is higher, the quantum efficiency of front side illuminated devices is lower, and the dynamic range is smaller than for CCDs. However, scientific CMOS devices are rapidly evolving and some disadvantages may be overcome in near future.

In order to characterize one of the current commercially available CMOS sensors, laboratory test with an Andor Neo camera were performed. The tests essentially confirmed the extraordinary low readout noise of ~2 electrons at 200MHz (for global shutter modes), the non-Gaussian distribution of the read noise (individual pixels are much noisier than the average) and the very limited dynamic range. The latter is limited to 600:1 in high gain and to 2'000:1 in low gain mode (higher dynamic ranges may be obtained in the somewhat problematic dual gain modes).

We conclude that optical observations of space objects may benefit from applying CMOS detectors, and that new observation concepts become feasible with these sensors. However, and in particular for observing faint objects, the currently applied techniques for CCDs need to be reconsidered in some areas.

5 REFERENCES

[1] Schildknecht, T., U. Hugentobler, and M. Ploner (1999), Optical Surveys of Space Debris in GEO, *Advances in Space Research*, **23** (1), pp. 45–54.

[2] Schildknecht, T., R.Musci, M. Ploner, G. Beutler,W. Flury, J. Kuusela, J. de Leon Cruz, and L. de Fatima Dominguez Palmero (2004), Optical Observations of Space Debris in GEO and in Highly-eccentric Orbits, A*dvances in Space Research*, **34** (5), pp. 901–911.

[3] Flohrer, T., T. Schildknecht, R. Musci, and E. Stöveken (2005), Performance estimation for GEO space surveillance, *Advances in Space Research*, **35**, pp. 1226–1235.

[4] Flohrer, T., T. Schildknecht, and R. Musci (2008), Proposed Strategies for Optical Observations in a Future European Space Surveillance Network, *Advances in Space Research*, **41**, pp. 1010–1021.

[5] Milani, A., D. Farnocchia, L. Dimare, A. Rossi, F. Bernardi (2012), Innovative observing strategy and orbit determination for Low Earth Orbit space debris, *Planetary and Space Science*, **62**,pp. 10-22.

[6] Flohrer, T., Krag, H., Klinkrad, H., and Schildknecht, T. (2011). Feasibility of performing space surveillance tasks with a proposed space-based optical architecture. *Advances in Space Research*, **47**(6), pp. 1029-1042.

[7] Flohrer, T., Schildknecht, T, Jehn, R. and Oswald, M. (2006), Performance of a Proposed Instrument for Space-based Optical Observation of Space Debris, in Proc. of the 57th International Astronautical Congress, Valencia, Spain, IAC-06-B6.1.01.

[8] Wokke, F. J. P., A. J. Kramer, R. van Benthem, R. B. Annes, T. Flohrer, T. Schildknecht, E. Stveken, E. Valtonen, J. Peltonen, E. Riihonen, T. Eronen, J. Kuusela, W. Flury, and R. Jehn (2006), An Instrumental Design for Space-based Optical Observation of Space Debris, in Space Debris and Space Traffic Management Symposium 2005, Vol. 112 of *AAS Science and Technologies Series*, edited by J. Bendisch, pp. 73–84, Univelt publishers, San Diego, USA.

[9] A. Gamal, Computational Image Sensors, IEEE International Conference of Computational Photography, (April 16-17, 2009).

[10] Scientific CMOS Technology. A High-Performance Imaging Breakthrough. http://www.scmos.com/files/high/scmos_white_paper_8mb.pdf.

[11] Neo and Zyla sCMOS Cameras. Imaging Without Compromise. http://www.andor.com/pdfs/literature/Andor_sCMOS_Brochure.pdf.

[12] Moore, A.C., Ninkov, Z. and Forrest, W.J.: Interpixel capacitance in nondestructive focal plane arrays. *Proc. SPIE 5167*, Focal Plane Arrays for Space Telescopes, **204** (2004).

[13] Finger, G. et al.: Conversion Gain and Interpixel Capacitance of CMOS Hybrid Focal Plane Arrays. *Scientific Detectors for Astronomy 2005*, p 477. Springer, Berlin (2006)